Stability of primary frequency control with on-off load side participation in power networks

Andreas Kasis, Nima Monshizadeh and Ioannis Lestas

Abstract— **We consider the problem of load side participation providing ancillary services to the power network within the primary frequency control timeframe. In particular, we consider on-off loads that switch when prescribed frequency thresholds are exceeded in order to assist existing primary frequency control mechanisms. However, such control policies are prone to chattering, which limits their practicality. To resolve this issue, we propose loads that follow a hysteretic on-off policy, and show that chattering behavior is not observed within such setting. Furthermore, we provide design conditions that ensure the existence of equilibria when such loads are implemented. However, as numerical simulations demonstrate, hysteretic loads may exhibit limit cycle behavior, which is undesirable. This is resolved by proposing a novel control scheme for hystertic loads. For the latter scheme, we provide asymptotic stability guarantees and show that no limit cycle or chattering will be exhibited. The practicality of our analytic results is demonstrated with numerical simulations on the Northeast Power Coordinating Council (NPCC) 140-bus system.**

I. Introduction

Motivation and literature review: Renewable sources of generation are expected to increase their penetration in power networks over the next years [1], [2]. This will result in increased intermittency in the generated power endangering power quality and potentially the stability of the power network. This encourages further study of the stability properties of the power grid.

Controllable loads are considered to be a way to counterbalance intermittent generation, due to their ability to provide fast response at urgencies by adapting their demand accordingly. The use of loads as ancillary services, in conjunction with a large penetration of renewable sources of generation will significantly increase the complexity of the network. This shows the need for distributed schemes that will guarantee the stability of the power network when some local conditions are satisfied. In recent years, various research studies considered controllable demand as a means to support primary [3], [4], [5], [6] and secondary [7], [8], [9], [10], frequency control mechanisms, with objectives to ensure that generation and demand are balanced and that frequency converges to its nominal value (50Hz or 60Hz) respectively.

On many occasions, loads are more realistically represented by a discrete set of possible demand values, e.g. on and off states, and hence a continuous representation does not suffice for their study. The possible on-off nature of loads has been pointed out in [11] (see also the extended version in [12]), which considered on-off loads that switched when some frequency deviation was reached in order to support the network at urgencies within the secondary frequency control timeframe. Furthermore, [13] considered two switching modes of operation for loads (at nominal and urgent situations), where controllable load inputs were determined from the local deviations in frequency. Moreover, the effect of frequency responsive on/off loads is demonstrated by simulations in [14]. Hence, the study of frequency dependent on-off loads that provide support to the power network is important for the development of demand response schemes. Furthermore, the fast response required to provide ancillary support at urgencies coincides with the primary frequency control timeframe, which makes its study highly relevant for this purpose.

Contribution: This paper extends the ideas of [11] to primary frequency control, considering frequency dependent on-off loads to provide ancillary service to the network at urgencies, when appreciable frequency deviations are experienced. The fact that the equilibrium frequency can be different from its nominal value within the primary frequency control timeframe makes the analysis significantly more complicated, introducing problems related with the existence of equilibria and the presence of limit cycles. We first show that the inclusion of loads that switch at a prescribed frequency does not compromise the stability of the power network, and results in enhanced frequency performance. However, such controllable loads may switch arbitrarily fast within a finite interval of time, or in other words, exhibit chattering behavior, which might limit their practicality. Inspired by [11], we consider on-off loads with hysteretic dynamics and show that chattering is no longer experienced. However, the existence of equilibria becomes a non-trivial issue when such loads are considered. We address this by providing design conditions that guarantee the existence of equilibria to the system. Furthermore, numerical simulations demonstrate that the inclusion of hysteretic loads can result to limit cycle behavior which is undesirable. To resolve this issue, we propose a novel distributed scheme for the control of hysteretic loads. Stability guarantees are again provided for this class of loads, and the absence of chattering and limit cycles are analytically proven. Finally, we provide a numerical validation of our results through a simulation on the NPCC 140-bus system, where it is demonstrated that the presence of frequency dependent on-off loads results in frequency response with significantly reduced overshoot.

Paper structure: The structure of the paper is as follows: Section II includes some basic notation and in section III we present the power network model. In section IV we consider controllable demand that instantaneously switches on/off whenever certain frequency thresholds are met and present our results concerning network stability. In section V, we consider controllable loads with hysteretic patterns and provide design conditions that guarantee the existence of equilibria when these loads are considered. In section VI, we propose a scheme to resolve the issue of potential limit cycle behavior from hysteretic loads and provide relevant asymptotic stability guarantees. Numerical investigations of the results are provided in section VII. Finally, conclusions are drawn in section VIII. Note that the proofs of the main results are omitted due to space constraints and will be provided in an extended version of this paper.

II. Notation

Real and natural numbers are denoted by $\mathbb{R}$ and $\mathbb{N}$ respectively, and the set of n-dimensional vectors with real entries is denoted by $\mathbb{R}^n$. We use $\mathbf{0}_n$ and $\mathbf{1}_n$ to denote $n \times 1$

This work was supported by ERC starting grant 679774.

Andreas Kasis and Ioannis Lestas are with the Department of Engineering, University of Cambridge, Trumpington Street, Cambridge, CB2 1PZ, United Kingdom; e-mails: ak647@cam.ac.uk, icl20@cam.ac.uk

Nima Monshizadeh is with the Engineering and Technology Institute, University of Groningen, Nijenborgh 4, 9747AG, Groningen, The Netherlands. email: n.monshizadeh@rug.nl

vectors with all elements equal to 0 and 1 respectively. For a discrete set Σ, let $|\Sigma|$ denote its cardinality. Moreover, let $\mathcal{B}(\mathbb{R}^n)$ denote the collection of subsets of $\mathbb{R}^n$.

III. Network model

We describe the power network model by a connected graph (N, E) where $N = \{1, 2, \dots, |N|\}$ is the set of buses and $E \subseteq N \times N$ the set of transmission lines connecting the buses. Furthermore, we use (i, j) to denote the link connecting buses i and j and assume that the graph (N, E) is directed with arbitrary direction, so that if $(i, j) \in E$ then $(j, i) \notin E$. For each $j \in N$, we use $i : i \to j$ and $k : j \to k$ to denote the sets of buses that are predecessors and successors of bus j respectively. It is important to note that the form of the dynamics in (1)–(2) below is unaltered by any change in the graph ordering, and all of our results are independent of the choice of direction. The following assumptions are made for the network:
1) Bus voltage magnitudes are $|V_j| = 1$ p.u. for all $j \in N$.
2) Lines $(i, j) \in E$ are lossless and characterized by their susceptances $B_{ij} = B_{ji} > 0$.
3) Reactive power flows do not affect bus voltage phase angles and frequencies.
4) Relative phase angles are sufficiently small such that the approximation $\sin \eta_{ij} = \eta_{ij}$ is valid.

We use swing equations to describe the rate of change of frequency at each bus. This motivates the following system dynamics (e.g. [15]),

$$\dot{\eta}_{ij} = \omega_i - \omega_j,\ (i, j) \in E, \tag{1a}$$

$$M_j \dot{\omega}_j = -p_j^L + p_j^M - (d_j^c + d_j^u) - \sum_{k:j\to k} p_{jk} + \sum_{i:i\to j} p_{ij}, j \in N, \tag{1b}$$

$$p_{ij} = B_{ij} \eta_{ij},\ (i, j) \in E. \tag{1c}$$

In system (1) the time-dependent variables p_j^M, d_j^c and ω_j represent, respectively, the mechanical power injection, the controllable load and the deviation from the nominal value[1] of frequency at bus j. The quantity d_j^u is also a time-dependent variable that represents the uncontrollable frequency-dependent load and generation damping present at bus j. Furthermore, the quantities[2] η_{ij} and p_{ij} are time-dependent variables that represent, respectively, the power angle difference, and the power transmitted from bus i to bus j. The constant $M_j > 0$ denotes the generator inertia. We study the response of system (1) at a step change in the uncontrollable demand p_j^L at each bus j.

A. Generation and uncontrollable demand dynamics

We shall consider generation and uncontrollable demand dynamics described by

$$\tau_j \dot{p}_j^M = -(p_j^M + \alpha_j \omega_j),\ j \in N, \tag{2a}$$

$$d_j^u = A_j \omega_j,\ j \in N, \tag{2b}$$

where $\tau_j > 0$ are time constants and $A_j > 0$ and $\alpha_j > 0$ for all $j \in N$ are damping and droop coefficients respectively.

Note that the analysis carried in this paper is still valid for more general generation/demand dynamics, including cases of nonlinear and higher order dynamics, provided certain input-output conditions hold, as shown in [5], [12]. We choose to use the simple first order generation and static uncontrollable demand dynamics for simplicity and to avoid a shift in the focus of the paper from on-off loads.

[1] A nominal value is defined as an equilibrium of (1) with frequency equal to 50Hz (or 60Hz).

[2] The phase angle differences between buses i and j, denoted by η_{ij}, must also satisfy $\eta_{ij} = \theta_i - \theta_j$, where $\dot{\theta}_i = \omega_i$. Hence the vector η belongs to the image of R^T, where R is the incidence matrix of the graph (N, E). This equation is omitted in (1) since power transfers are functions of the phase differences only.

IV. On-Off controllable loads

Within this section, we shall consider frequency dependent on-off loads that respond to frequency deviations by switching to an appropriate state in order to aid the network at urgencies.

The considered controllable demand dynamics are described by the discontinuous map $f_j^c : \mathbb{R} \to \mathbb{R}$ defined as

$$d_j^c = f_j^c(\omega_j) = \begin{cases} \overline{d}_j, & \omega_j > \overline{\omega}_j, \\ 0, & \underline{\omega}_j < \omega_j \leq \overline{\omega}_j, \\ \underline{d}_j, & \omega_j \leq \underline{\omega}_j, \end{cases} \quad j \in N, \tag{3}$$

where $-\infty < \underline{d}_j \leq 0 \leq \overline{d}_j < \infty$, and $\overline{\omega}_j > 0 > \underline{\omega}_j$ for all $j \in N$. Note that the dynamics in (3) may be trivially extended to include more discrete values, that would possibly respond to higher frequency deviations. The extension has been omitted for simplicity.

Analysis of the discontinuous dynamics in (3) may be performed by employing Filippov solutions, following the definition in [16]. Note that the employment of Filippov solutions is common in the analysis of discontinuous systems. Hence, it will be convenient to represent the dynamics of (3) using a Filippov set valued map [16] as follows:

$$F[d_j^c] = \begin{cases} [0, \overline{d}_j], & \omega_j = \overline{\omega}_j \\ [\underline{d}_j, 0], & \omega_j = \underline{\omega}_j, \\ \{f_j^c(\omega_j)\}, & \text{otherwise}, \end{cases} \quad j \in N. \tag{4}$$

The states of the interconnected system (1)–(3) are denoted by $x = (\eta, \omega, p^M)$, where any variable without subscript represents a vector with all respective components. For a compact representation of this system, consider the Filippov set valued map $Q : \mathbb{R}^n \to \mathcal{B}(\mathbb{R}^n)$, where $n = |E| + 2|N|$, such that

$$\dot{x} \in Q(x) \tag{5}$$

where

$$Q(x) := \begin{cases} \{\omega_i - \omega_j\},\ (i, j) \in E, \\ \{\frac{1}{M_j}(-p_j^L + p_j^M - A_j\omega_j - v_j - \sum_{k:j\to k} p_{jk} \\ + \sum_{i:i\to j} p_{ij}) : v_j \in F[d_j^c]\}, j \in N, \\ \{-\frac{1}{\tau_j}(p_j^M + \alpha_j \omega_j)\},\ j \in N. \end{cases}$$

This representation allows the discontinuous frequency derivatives to be well defined at all points.

A. Equilibrium and solutions analysis

Due to added complexity in the analysis, as a result of the discontinuous dynamics in (3), notions such as equilibrium and solution need to be well defined and explained in this context. We shall first study the equilibria of this system and then its solutions.

We now describe what is meant by an equilibrium of the interconnected system (5).

Definition 1: The constant $x^* = (\eta^*, \omega^*, p^{M,*})$ defines an equilibrium of the system (5) if $0_n \in Q(x^*)$.

Note that the corresponding equilibrium value of the vector $d^{u,*}$ follows directly from ω^*. Similarly the steady state controllable demand $d^{c,*}$ satisfies $d_j^{c,*} \in F[d_j^c](\omega_j^*), j \in N$. Furthermore, note that an equilibrium of (5) always exists.

In order to study the behavior of (1)–(3), it is necessary to demonstrate the existence of solutions to it, which is addressed in the following Lemma.

Lemma 1: There exists a Filippov solution of (1)–(3) from any initial condition $x_0 = (\eta(0), \omega(0), p^M(0)) \in \mathbb{R}^n$.

B. Convergence analysis

This section contains the main result of this section.

Theorem 1: The Filippov solutions of (1)–(3) converge for all initial conditions to a set of equilibria, as defined in Definition 1.

The above theorem shows that all Filippov solutions of the system (1)–(3) asymptotically converge to the set of equilibria of the system. It therefore demonstrates that the inclusion of controllable loads with dynamics described by (3) does not compromise the stability of the system.

C. Chattering

A possibility when discontinuous systems are involved, is the occurrence of infinitely many switches within some finite time, a phenomenon known as chattering (e.g. [17]). Such behavior might not be acceptable in practical implementations and is preferable to be avoided.

Chattering may occur in controllable loads, as shown in simulations. The reason of such behavior is that the frequency derivative might change sign when passing a discontinuity, making the vector field to point towards the discontinuity and hence frequency to stay at that particular value. For instance, when $0 < M_j \dot{\omega}_j < \overline{d}_j$ at some time instant where $\omega_j = \overline{\omega}_j$ then $\dot{\omega}_j < 0$ when the switch occurs which in turn cause frequency to decrease. This change in derivative sign will cause an infinite amount of switches within some finite time, resulting to the aforementioned chattering behavior.

V. Hysteresis on controllable loads

In this section we discuss how on-off load dynamics might be modified in order to ensure that no chattering will be experienced. We propose the use of hysteresis dynamics such that controllable loads switch on when a particular frequency is reached and off at a different frequency that is closer to the nominal. Such dynamics may be described by

$$d^c_j = \overline{d}_j \sigma_j, \quad \sigma_j(t^+) \in \begin{cases} \{1\}, & \omega_j > \omega^1_j \\ \{0\}, & \omega_j < \omega^0_j \\ \{\sigma_j(t)\}, & \omega^0_j < \omega_j < \omega^1_j \\ \{0, \sigma_j\}, & \omega_j = \omega^0_j \\ \{\sigma_j, 1\}, & \omega_j = \omega^1_j \end{cases} \tag{6}$$

where $j \in N$, $t^+ = \lim_{\epsilon \to 0}(t+\epsilon)$, $\overline{d}_j > 0$ and the frequency thresholds ω^0_j, ω^1_j, satisfy $\omega^1_j > \omega^0_j > 0$. Furthermore, $\sigma_j, j \in N$ denotes the discrete state at bus j and σ the vector with elements $\sigma_j \in P$ for all $j \in N$, where $P = \{0, 1\}$. For generality, the control scheme (6) considers two possibilities when frequency thresholds ω^0_j and ω^1_j are reached, corresponding to a switch when the frequency reaches or passes a particular threshold. This approach is used throughout the rest of the paper and is consistent with the widely used framework in [18] for the analysis of hybrid systems. Note that the results in Sections V and VI concerning convergence of solutions and absence of chattering are about all solutions of the resulting hybrid systems.

The dynamics in (6) describe loads that switch ON from OFF. Note that the conjugate case of loads switching OFF from ON can also be incorporated by reversing the signs of frequency thresholds and controllable demand deviations and that all the analytic results of this paper can be trivially extended to include this case. However, we consider only loads that switch from OFF to ON for simplicity in presentation. Moreover, we let $t_{i,j}, i \in \mathbb{N}, j \in N$ denote the time-instants where the value of σ_j changes. Within the rest of the paper we shall adopt the notation $a^+ = a(t^+)$ for any vector $a(t) \in \mathbb{R}^m, m > 0$.

The behavior of system (1),(2),(6) can be described by the states $z = (x, \sigma)$, where $x = (\eta, \omega, p^M) \in \mathbb{R}^n$, $n = |E| + 2|N|$, is the continuous state, and $\sigma \in P^{|N|}$ the discrete state. Moreover, let $\Lambda = \mathbb{R}^n \times P^{|N|}$ be the space where the system's states evolve. The continuous dynamics of the system (1),(2),(6) can be described by

$$\dot{\eta}_{ij} = \omega_i - \omega_j, \ (i,j) \in E, \tag{7a}$$

$$M_j \dot{\omega}_j = -p^L_j + p^M_j - (\overline{d}_j \sigma_j + A_j \omega_j) - \sum_{k:j\to k} p_{jk} + \sum_{i:i\to j} p_{ij}, \ j \in N, \tag{7b}$$

$$p_{ij} = B_{ij} \eta_{ij}, \ (i,j) \in E, \tag{7c}$$

$$\tau_j \dot{p}^M_j = -(p^M_j + \alpha_j \omega_j), \ j \in N, \tag{7d}$$

$$\dot{\sigma}_j = 0, j \in N, \tag{7e}$$

which is valid when z belongs to the set C described below.

$$C = \{z \in \Lambda : \sigma_j \in \mathcal{I}_j(\omega_j), \ \forall j \in N\} \tag{8}$$

where

$$\mathcal{I}_j(\omega_j) = \begin{cases} \{1\}, & \omega_j > \omega^1_j, \\ \{0\}, & \omega_j < \omega^0_j, \\ \{0, 1\}, & \omega^0_j \le \omega_j \le \omega^1_j. \end{cases}$$

Alternatively, when z belongs to the set $D = \Lambda \setminus C \cup \underline{D}$ where $\underline{D} = \{z \in \Lambda : \sigma_j \in \mathcal{I}^D_j(\omega_j), \ \forall j \in N\}$, and

$$\mathcal{I}^D_j(\omega_j) = \begin{cases} \{0\}, & \omega_j = \omega^1_j, \\ \{1\}, & \omega_j = \omega^0_j, \end{cases}$$

then its components follow the discrete update depicted below

$$x^+ = x, \qquad \sigma_j(t^+) = \begin{cases} 1, & \omega_j \ge \omega^1_j, \\ 0, & \omega_j \le \omega^0_j. \end{cases} \tag{9}$$

We can now provide the following compact representation for the hybrid system (1),(2),(6),

$$\dot{z} = f(z), z \in C, \quad z^+ = g(z), z \in D, \tag{10}$$

where $f(z) : C \to \Lambda$ and $g(z) : D \to C$ are described by (7) and (9) respectively. Note that $z^+ = g(z)$ represents a discrete dynamical system where z^+ indicates that the next value of the state z is given as a function of its current value through $g(z)$. Moreover, note that $C \cup D = \Lambda$.

A. Analysis of equilibria and solutions

In this subsection, we define and study the equilibria and solutions of (10). We provide necessary and sufficient design conditions for the existence of equilibria of (10) and show that the hysteretic dynamics resolve any chattering issues.

Below, we provide a definition of an equilibrium of a system described by (10).

Definition 2: A point z^* is an equilibrium of the system described by (10) if it satisfies $f(z^*) = 0, z^* \in C$ or $z^* = g(z^*), z^* \in D$.

The presence of hysteretic dynamics makes the existence of equilibria of (10) a non-trivial issue. The following theorem provides necessary and sufficient conditions for the existence of an equilibrium for (10).

Theorem 2: An equilibrium point z^* of (10) exists for any p^L if $\omega^1_j - \omega^0_j \ge \overline{d}_j / \sum_{i \in N}(A_i + \alpha_i)$, holds for all $j \in N$.

Theorem 2 provides a design condition on the hysteretic dynamics which ensures that equilibria will exist for any load profile. Potential lack of equilibria results in undesirable behavior types such as limit cycles. Stability-wise, the conditions for existence of equilibria can be seen as necessary conditions for convergence to some fixed point. Furthermore, there exist configurations where it can be shown that the condition in Theorem 2 is also necessary, e.g. when the hysteresis region in at least one load is non-overlapping with the respective hysteresis regions of other loads.

The existence of solutions[3] to (10) as well as of a finite dwell time between switches of states σ_j within any compact set are shown by the following lemma.

Lemma 2: For any initial condition $z(0,0) \in \Lambda$ there exists a complete solution of (10). Furthermore, for any complete bounded solution of (10), there exists $\tau_j > 0$ such that $\min_{i\geq 1}(t_{i+1,j} - t_{i,j}) \geq \tau_j$ for any $j \in N$.

Remark 1: The importance of Lemma 2 is that it shows that no chattering will occur for any complete bounded solution of system (10). This is because for any finite time interval $\tau = \min_j \tau_j, j \in N$, the vector σ changes at most $|N|$ times, as follows from the Lipschitz property of the vector fields and the fact that after a switch occurs at bus j then frequency needs to change by at least $|\omega_j^1 - \omega_j^0|$ for a new switch to occur. This shows the practical advantage of (10) when compared to (5).

B. Limit cycle behavior

Numerical simulations demonstrate that limit cycle behavior can be obtained when the considered hysteretic loads are introduced in the network (see Section VII). This is a consequence of the load ON-OFF behavior which results in discontinuous changes in the vector field which in turn cause further switches. Practically, switching will eventually cease due to actions related to secondary frequency regulation (see [11]). However, such behavior is considered undesirable for practical implementations. In the following section we present an approach to resolve this issue.

VI. A novel scheme for hysteretic loads

To overcome the issue of limit cycles, we adapt the scheme in (6) by introducing an additional input to the discrete state which governs whether a load is allowed to switch back to its nominal operation. We then explain how this additional input needs to be designed so that asymptotic stability can be guaranteed. In particular, we consider the following scheme for controllable demand dynamics

$$d_j^c = \overline{d}_j \sigma_j, \quad \sigma_j(t^+) \in \begin{cases} \{1\}, & \omega_j > \omega_j^1 \\ \{0\}, & \omega_j < \omega_j^0 \text{ and } p_j^c < \underline{p}_j^c \\ \{\sigma_j(t)\}, & \begin{cases} \omega_j^0 < \omega_j < \omega_j^1 \\ \omega_j < \omega_j^0 \text{ and } p_j^c > \underline{p}_j^c \end{cases} \\ \{0, \sigma_j\}, & \begin{cases} \omega_j = \omega_j^0 \text{ and } p_j^c \leq \underline{p}_j^c \\ \omega_j \leq \omega_j^0 \text{ and } p_j^c = \underline{p}_j^c \end{cases} \\ \{\sigma_j, 1\}, & \omega_j = \omega_j^1 \end{cases} \tag{11}$$

where $j \in N$, $\underline{p}_j^c$ are variables available for design (see below), $\overline{d}_j, \omega_j^0$ and ω_j^1 are as in (6) and p_j^c is a power command variable given by

$$\gamma_{ij} \dot{\psi}_{ij} = p_i^c - p_j^c, \ (i,j) \in \tilde{E} \tag{12a}$$

$$\gamma_j \dot{p}_j^c = -p_j^L - p_j^c - \sum_{k:j\to k} \psi_{jk} + \sum_{i:i\to j} \psi_{ij}, \ j \in N, \tag{12b}$$

where $\tilde{E}$ denotes the links of an implicit connected communication graph, and the variable ψ_{ij} is a state of the controller that integrates the difference of power command variables between communicating buses i and j. Moreover, the power command and frequency thresholds $\underline{p}_j^c$ and ω_j^0 are assumed to satisfy the following condition.

Assumption 1: The values of $\underline{p}_j^c$ and ω_j^0 are chosen such that $\underline{p}_j^c < \mathcal{K}\omega_j^0$ holds, where $\mathcal{K} = \sum_{j\in N}(A_i + \alpha_i)/|N|$.

Remark 2: The scheme presented in (11) introduces an additional feedback on controllable loads from synchronizing power command variables. In particular, when the power command values are above their local respective thresholds $\underline{p}_j^c$, then switching from ON to OFF is prohibited. When the alternative case is considered at equilibrium, i.e. when $p_j^{c,*} \leq \underline{p}_j^c$, and therefore switching depends on frequency only, as follows from (11), then Assumption 1 guarantees that the respective frequency thresholds ω_j^0 are greater than the equilibrium frequency, which suffices to show the absence of limit cycles. The condition follows by noting that the equilibrium values of frequency and power command depend directly on the value of $\sum_{j\in N} p_j^L$, as shown below.

$$p^{c,*} = \frac{\sum_{j\in N}(-p_j^L)}{|N|} \tag{13a}$$

$$\omega^* = \frac{\sum_{j\in N}(-p_j^L - \overline{d}_j\sigma_j^*)}{\sum_{j\in N}(A_i + \alpha_i)} \tag{13b}$$

From (13b), it follows that the value of p^L suffices to obtain an upper bound on the equilibrium frequency, obtained when $\sigma^* = 0$, which allows it to be compared to the equilibrium value of power command. Then $\mathcal{K}$ follows simply as $\mathcal{K} = \frac{p^{c,*}}{\omega^*}\big|_{\sigma^*=0}$. Note that the condition can be easily fulfilled since both ω_j^0 and $\underline{p}_j^c$ are design variables. It should further be noted that Assumption 1 requires knowledge of the aggregate droop and damping coefficients from all buses across the network. However, for the purpose of the analysis, it is sufficient to have a lower bound to this value, which offers robustness to model uncertainty.

The behavior of system (1),(2),(11),(12) can be described by the states $\zeta = (\overline{x}, \sigma)$, where $\overline{x} = (x, p^c, \psi)$ and $\zeta \in M := \Lambda \times \mathbb{R}^{|N|+|\tilde{E}|}$. The continuous dynamics of the system (1),(2),(11),(12) can be described by (7) and (12) which are valid when ζ belongs to the set $\overline{C}$ described below.

$$\overline{C} = \{\zeta \in M : \sigma_j \in \mathcal{J}_j(\omega_j, p_j^c), \ \forall j \in N\} \tag{14}$$

where

$$\mathcal{J}_j(\omega_j, p_j^c) = \begin{cases} \{1\}, & \omega_j > \omega_j^1, \\ \{0\}, & \begin{cases} \omega_j < \omega_j^0 \text{ and } p_j^c \leq \underline{p}_j^c, \\ \omega_j \leq \omega_j^0 \text{ and } p_j^c < \underline{p}_j^c, \end{cases} \\ \{0, 1\}, & \begin{cases} \omega_j^0 \leq \omega_j \leq \omega_j^1, \\ \omega_j \leq \omega_j^0 \text{ and } p_j^c \geq \underline{p}_j^c. \end{cases} \end{cases}$$

Alternatively, when ζ belongs to the set $\overline{D} = M \setminus \overline{C} \cup \tilde{D}$ where $\tilde{D} = \{\zeta \in M : \sigma_j \in \mathcal{I}_j^D(\omega_j, p_j^c), \ \forall j \in N\}$, and

$$\mathcal{I}_j^D(\omega_j, p_j^c) = \begin{cases} \{0\}, & \omega_j = \omega_j^1, \\ \{1\}, & \begin{cases} \omega_j \leq \omega_j^0 \text{ and } p^c = \underline{p}_j^c, \\ \omega_j = \omega_j^0 \text{ and } p^c \leq \underline{p}_j^c, \end{cases} \end{cases}$$

then its components follow the discrete update depicted below,

$$\overline{x}^+ = \overline{x}, \quad \sigma_j(t^+) = \begin{cases} 1, & \omega_j \geq \omega_j^1, \\ 0, & \omega_j \leq \omega_j^0 \text{ and } p_j^c \leq \underline{p}_j^c. \end{cases} \tag{15}$$

[3] We use the definition of hybrid solutions from [18, Chapter 2].

We can now provide the following compact representation for the hybrid system (1),(2),(11),(12)

$$\dot{\zeta} = \overline{f}(\zeta), \zeta \in \overline{C}, \tag{16a}$$

$$\zeta^+ = \overline{g}(\zeta), \zeta \in \overline{D}, \tag{16b}$$

where $\overline{f}(\zeta) : \overline{C} \to M$ and $\overline{g}(\zeta) : \overline{D} \to \overline{C}$ are described by (7) and (12), and (15) respectively. Note that $\overline{C} \cup \overline{D} = M$ and $\overline{C} \cap \overline{D} = \tilde{D}$. Furthermore, note that both $\overline{C}$ and $\overline{D}$ are closed, as required in [18, Ass. 6.5, Th. 6.30] for (16) to be well-posed.

A. Analysis of equilibrium and solutions

Below we provide an equilibrium definition for (16).

Definition 3: A point ζ^* is an equilibrium of the system described by (16) if it satisfies $\overline{f}(\zeta^*) = 0, \zeta^* \in \overline{C}$ or $\zeta^* = \overline{g}(\zeta^*), \zeta^* \in \overline{D}$.

The following proposition demonstrates the existence and characterizes the equilibria of (16).

Proposition 1: Consider the system described by (16) and let Assumption 1 hold. Then, an equilibrium point always exists and satisfies $\zeta^* \in \overline{C}$.

Proposition 1 demonstrates the existence of equilibria to (16) when Assumption 1 holds. Note that although the condition in Theorem 2 is no longer required, its fulfilment is still a good practice along the on-off loads described by (11), allowing the existence of equilibria in case of malfunction or failure in the implementation of the p^c dynamics. The existence of solutions to (16) as well as that no chattering occurs are shown by the following proposition.

Proposition 2: For any initial condition $\zeta(0,0) \in M$ there exists a complete solution of (16). Furthermore, for any complete bounded solution of (16), there exists $\tau_j > 0$ such that $\min_{i \geq 1}(t_{i+1,j} - t_{i,j}) \geq \tau_j$ for any $j \in N$.

The importance of Proposition 2 is that it shows the existence of solutions to (16), which allows their analysis and that it also demonstrates a minimum time between consecutive switches, which shows that no chattering behavior will be experienced.

B. Stability of hybrid system

In this section, we provide our main stability result about system (16).

Theorem 3: Let Assumption 1 hold. Then the solutions of (16) converge for all initial conditions to the set of equilibria of (16), described by Definition 3.

Theorem 3 demonstrates the convergence of solutions to some equilibrium point of (16), described by Definition 3. Together with Proposition 2 it demonstrates that the inclusion of loads with dynamics described by (11), does not compromise the stability of the system and neither exhibits any chattering or limit cycle behavior.

VII. Simulation on the NPCC 140-bus system

In this section we verify our analytic results with a numerical simulation on the Northeast Power Coordinating Council (NPCC) 140-bus interconnection system, using the Power System Toolbox [19]. This model is more detailed and realistic than our analytical one, including line resistances, a DC12 exciter model, a subtransient reactance generator model, and turbine governor dynamics[4].

The test system consists of 93 load buses serving different types of loads including constant active and reactive loads and 47 generation buses. The overall system has a total real power of 28.55GW. For our simulation, we added five loads

[4]The details of the simulation models can be found in the Power System Toolbox data file datanp48.

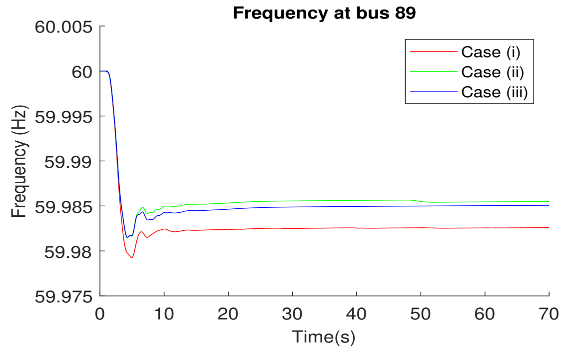

Fig. 1. Frequency at bus 89 with controllable load dynamics as in the following three cases: i) Switching case, ii) Hysteresis case, iii) Secure hysteresis case.

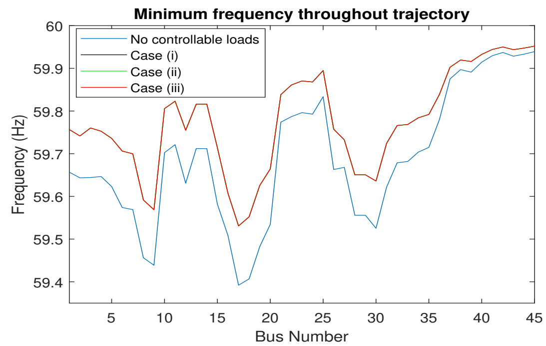

Fig. 2. Largest frequency overshoot for buses $1 - 45$ for four cases: i) Switching case, ii) Hysteresis case, iii) Secure hysteresis case, iv) No controllable loads case.

on units $2, 8, 9, 16$ and 17, each having a step increase of magnitude 3 p.u. (base 100MVA) at $t = 1$ second.

Controllable demand was considered within the simulations on 20 generation and 20 load buses, with loads controlled every 10ms.

The system was tested at three different cases. In case (i) controllable on-off loads with dynamics as in (3) were considered. The values for $\overline{\omega}_j$ were selected from a uniform distribution within the range $[0.02\ 0.07]$ and those of $\underline{\omega}_j$ by following $\underline{\omega}_j = -\overline{\omega}_j$. In case (ii) controllable loads with hysteretic dynamics described by (6) were considered. To have a fair comparison, the same frequency thresholds as in case (i) were used, with $\omega^1_j = \overline{\omega}_j$ and $\omega^0_j = \omega^1_j/2$. Finally, in case (iii), hysteretic loads following the dynamics in (11) were included. For this case, the same frequency thresholds as in case (ii) where used, where power command thresholds were chosen such that Assumption 1 was satisfied. For all cases $\overline{d} = 0.2p.u.$ was used. We shall refer to cases (i), (ii), and (iii) as the 'switching', 'hysteresis' and 'secure hysteresis' cases respectively.

The frequency at bus 89 for the three tested cases is shown in Fig. 1. From this figure, we observe that frequency converges to some constant value at all cases. Note that a smaller steady state frequency deviation is observed when hysteretic loads are considered, since the hysteresis allows more loads to stay switched at steady state. Moreover, Fig. 2 demonstrates that the inclusion of on-off loads decreases the maximum overshoot in frequency, by comparing the largest deviation in frequency with and without on-off controllable loads at buses $1 - 45$, where frequency overshoot was seen to be the largest. Note that the same overshoot profiles are observed in all cases (i), (ii), and (iii) since the same frequency thresholds have been used.

Furthermore, from Fig. 3 it can be seen that in case (i) controllable loads switch very fast, as demonstrated by the thick blue lines, indicating chattering behavior, where

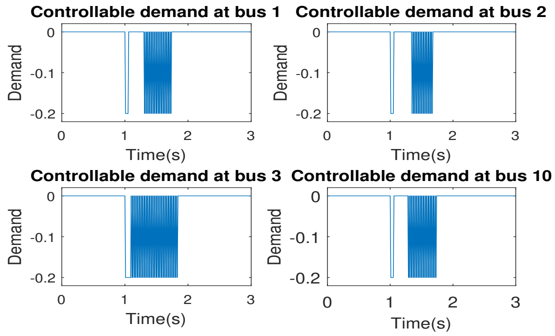

Fig. 3. Controllable demand at 4 buses with Switching on-off loads.

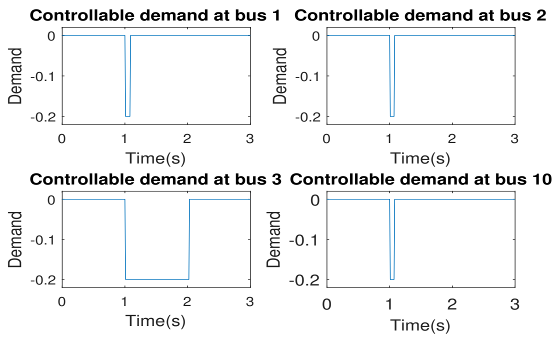

Fig. 4. Controllable demand at 4 buses with Hysteresis on-off loads.

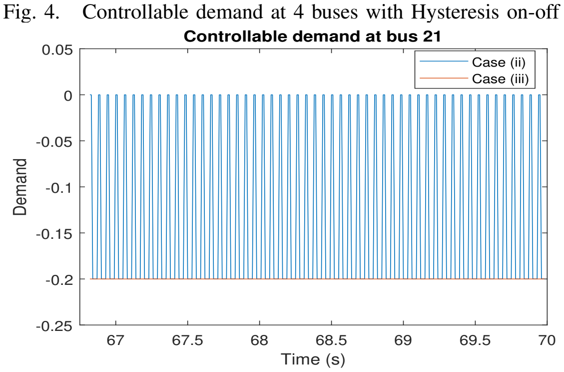

Fig. 5. Controllable demand at bus 21 for cases (ii) and (iii).

in case (ii) such behavior is not observed[5], since far less switches are exhibited, as shown in Figure 4. Both figures depict the behavior at the 4 buses where the fastest switches in hysteretic schemes have been observed. The chattering behavior in case (i) is also verified numerically since it was seen that for each of the 20 controllable loads the minimum time between consecutive switches was 10ms, which is the smallest time increment in our discrete numerical simulation. Therefore, the numerical results support the analysis of this paper, verifying that hysteresis eliminates chattering at controllable loads.

To demonstrate the possibility of existence of limit cycles when case (ii) is considered, we altered the frequency thresholds of the on-off load at bus 21 to make the upper one coincide with the equilibrium frequency and then repeated the simulations for cases (ii) and (iii). As demonstrated on Fig. 5, the load at bus 21 exhibits limit cycle behavior at steady state, whereas when the secure hysteresis scheme was considered, no such behavior was observed.

VIII. Conclusion

We have considered the problem of primary frequency control where controllable on-off loads provide ancillary services. We first considered loads that switch on when some frequency threshold is reached and off otherwise and provided relevant stability guarantees for the power network. Furthermore, it is discussed that such schemes might exhibit arbitrarily fast switching, which might limit their practicality. To cope with this issue, on-off loads with hysteretic dynamics were considered and it has been shown that such loads do not exhibit any chattering behavior. Furthermore, necessary and sufficient design conditions that guarantee the existence of equilibria when such loads are considered are provided. However, numerical simulations demonstrate that such loads may exhibit limit cycle behavior. As a remedy to this problem, we proposed a new control scheme that allows such loads to be included in the power network without compromising power network stability nor inducing any limit cycle behavior. Hence, such schemes are usable for practical implementations. Our analytic results have been verified with numerical simulations on the NPCC 140-bus system where it was shown that the presence of on-off loads reduces the frequency overshoot and that hysteresis schemes resolve issues caused by chattering. Furthermore, simulation results demonstrate that our proposed hysteretic scheme resolves issues related with limit cycle behavior. Interesting potential extensions in the analysis include incorporating more advanced on-off load dynamics and voltage dynamics.

[5]Note that analogous behavior to case (ii) has been observed for case (iii). These results are omitted for compactness in presentation.

References

[1] H. Lund, "Large-scale integration of optimal combinations of pv, wind and wave power into the electricity supply," *Renewable energy*, vol. 31, no. 4, pp. 503–515, 2006.

[2] A. Ipakchi and F. Albuyeh, "Grid of the future," *IEEE power and energy magazine*, vol. 7, no. 2, pp. 52–62, 2009.

[3] A. Molina-Garcia, F. Bouffard, and D. S. Kirschen, "Decentralized demand-side contribution to primary frequency control," *IEEE Transactions on Power Systems*, 2011.

[4] S. Trip and C. De Persis, "Optimal generation in structure-preserving power networks with second-order turbine-governor dynamics," in *Control Conference (ECC), 2016 European*, pp. 916–921, IEEE, 2016.

[5] A. Kasis, E. Devane, C. Spanias, and I. Lestas, "Primary frequency regulation with load-side participation part i: stability and optimality," *IEEE Transactions on Power Systems*, 2016.

[6] E. Devane, A. Kasis, M. Antoniou, and I. Lestas, "Primary frequency regulation with load-side participation part ii: beyond passivity approaches," *IEEE Transactions on Power Systems*, vol. 32, 2017.

[7] E. Mallada, C. Zhao, and S. Low, "Optimal load-side control for frequency regulation in smart grids," in *Communication, Control, and Computing (Allerton), 2014 52nd Annual Allerton Conference on*, pp. 731–738, IEEE, 2014.

[8] S. Trip, M. Bürger, and C. De Persis, "An internal model approach to frequency regulation in inverter-based microgrids with time-varying voltages," in *Decision and Control (CDC), 2014 IEEE 53rd Annual Conference on*, pp. 223–228, IEEE, 2014.

[9] A. Kasis, E. Devane, and I. Lestas, "Stability and optimality of distributed schemes for secondary frequency regulation in power networks," in *IEEE 55th Conference on Decision and Control (CDC)*, pp. 3294–3299, IEEE, 2016.

[10] A. Kasis, N. Monshizadeh, and I. Lestas, "A novel distributed secondary frequency regulation scheme for power networks with high order turbine governor dynamics," *17th European Control Conference, 2018, (extended version on arXiv:1806.11449)*.

[11] A. Kasis, N. Monshizadeh, and I. Lestas, "Secondary frequency regulation in power networks with on-off load side participation," in *Decision and Control (CDC), 2017 IEEE 56th Annual Conference on*, pp. 5702–5707, IEEE, 2017.

[12] A. Kasis, N. Monshizadeh, and I. Lestas, "Secondary frequency control with on-off load side participation in power networks," *arXiv preprint arXiv:1708.09351*, 2017.

[13] T. Liu, D. J. Hill, and C. Zhang, "Non-disruptive load-side control for frequency regulation in power systems," *IEEE Transactions on Smart Grid*, vol. 7, no. 4, pp. 2142–2153, 2016.

[14] N. Lu *et al.*, "Design considerations for frequency responsive grid friendly tm appliances," in *Transmission and Distribution Conference and Exhibition, 2005/2006 IEEE PES*, pp. 647–652, IEEE, 2006.

[15] A. R. Bergen and V. Vittal, *Power Systems Analysis*. Prentice Hall, 1999.

[16] J. Cortes, "Discontinuous dynamical systems," *IEEE Control Systems*, vol. 28, no. 3, 2008.

[17] A. Levant, "Chattering analysis," *IEEE transactions on automatic control*, vol. 55, no. 6, pp. 1380–1389, 2010.

[18] R. Goebel, R. G. Sanfelice, and A. R. Teel, *Hybrid Dynamical Systems: modeling, stability, and robustness*. Princeton University Press, 2012.

[19] K. Cheung, J. Chow, and G. Rogers, "Power system toolbox, v 3.0," *Rensselaer Polytechnic Inst. and Cherry Tree Sc. Software*, 2009.